Composite Structures 197 (2018) 72–79

Contents lists available at ScienceDirect

Composite Structures

journal homepage: www.elsevier.com/locate/compstruct

Torsional buckling of graphene platelets (GPLs) reinforced functionally graded cylindrical shell with cutout

Yu Wang[a], Chuang Feng[a,*], Zhan Zhao[a], Fangzhou Lu[b], Jie Yang[a,*]

[a] School of Engineering, RMIT University, Bundoora, VIC 3083, Australia
[b] State Key Laboratory of Mechanics and Control of Mechanical Structures, Nanjing University of Aeronautics and Astronautics, Nanjing 210016, PR China

ARTICLE INFO

Keywords:
Torsional buckling
Functionally graded material
Graphene platelets
Cylindrical shell

ABSTRACT

This paper studies the torsional buckling of functionally graded cylindrical shells reinforced with graphene platelets (GPLs) through finite element method (FEM). The cylindrical shell is consisted of a number of layers in the thickness direction, in which the GPL concentration varies from layer to layer. The Young's modulus and Poisson's ratio of the composites are determined by Halpin-Tsai model and rule of mixture, respectively. The FEM model is validated by comparing present results with theoretical predictions for homogeneous shells. Parametric study is carried out to investigate the effects of the number of layers, the GPL distribution patterns, the dimensions of shell, the weight fraction and size of GPLs, and the existence of cutout on torsional buckling. The results demonstrate using multi-layers is accurate enough to obtain functionally graded structures. GPL distribution plays a significant role in the buckling. Increasing the number of layers significantly decreases the stress gradient between two adjacent layers. Square shaped GPLs with fewer layers are preferred as reinforcements. With the increase of cutout size, the buckling load decreases and the structure undergoes the transition from global to local buckling mode. Moreover, the effects of the slenderness, orientation and position of the cutout on buckling are examined.

1. Introduction

The ability to reduce delamination and inhibit crack propagation [1,2] has been increasingly promoting the potential application of functionally graded materials (FGMs) in various engineering areas, such as aerospace [3], automotive [4] and mechanical engineering [5] since they were proposed in 1984. FGMs are composed of two or more constituent materials, in which the material composition and properties vary gradually along one or more directions. Their unique attributes produce the smooth variation of material properties, i.e. Young's modulus, Poisson's ratio and mass density, which can reduce the interfacial stress mismatch between two dissimilar materials. Recently, using carbon-based reinforcements, i.e. carbon fibres (CFs) [6–8], carbon blacks (CBs) [9] and carbon nanotubes (CNTs) [10–13], in polymer composites to produce FGMs has drawn tremendous attention from both academic and industrial communities.

Recently, graphene and its derivatives, i.e. graphene platelets (GPLs) and graphene oxide (GO), demonstrate great potentials as reinforcements to develop high performance composites and FGM structures. This can be attributed to graphene and its derivatives' prominent mechanical and physical properties as well as their unique two-dimensional feature and extremely large surface area, leading to better load transfer between polymer matrix and reinforcements [14,15]. Extensive research work has been implemented on graphene reinforced composite materials. Park et al. [16] experimentally observed impressive toughening effects of graphene on epoxy. Rafiee et al.'s work [17] demonstrated that the Young's modulus could be boosted by 31% by dispersing 0.1 wt% of GPLs into epoxy. A nearly 10-folds improvement in Young's modulus and 150% increase in tensile strength were also achieved by Zhao et al. [18] by incorporating 1.8 vol% of fully exfoliated graphene nanosheets with poly(vinyl alcohol). Apart from experimental tests, the remarkable enhancing effects of graphene and graphene-derived materials are also verified by molecular dynamics (MD) simulations [19–21], finite element analysis (FEA) [22,23] and micromechanics modelling [24–27].

In addition to the focus on material properties, researchers are now developing graphene reinforced FGM structures. Feng et al. [28,29] proposed a multilayer FGM beam reinforced by GPLs and analysed its bending and vibration behaviours. Yang et al. [30] used first-order shear deformation theory to study the buckling and postbuckling of the nanocomposite beam. Considering temperature effect, Wu et al. [31] studied the thermal buckling and postbuckling behaviours of the

* Corresponding authors.
E-mail addresses: chuang.feng@rmit.edu.au (C. Feng), j.yang@rmit.edu.au (J. Yang).

https://doi.org/10.1016/j.compstruct.2018.05.056
Received 5 February 2018; Received in revised form 6 May 2018; Accepted 9 May 2018
0263-8223/

graphene reinforced nanocomposite plates. More work on graphene reinforced FGM beam and plates can also be found in [32–38]. Cylindrical shell is another key component that has broad applications in various engineering fields, such as aerospace engineering, civil engineering and mechanical engineering. During the lifecycle of cylindrical shells, one of the most critical problems that constrain their load bearing capacity is stability [39–41]. Currently, lots of research work has been conducted to investigated the buckling behaviours of cylindrical shells by experimental tests [42,43], theoretical methods [44,45] and finite element analysis [46,47]. However, most of the work is mainly focused on the buckling performances under axially loaded compression. Torsional buckling is another typical stability issue for cylindrical shell structures. Donnell et al. [48], Batdorf et al. [49] and Timoshenko et al. [50] proposed theoretical formulas to obtain approximate solutions to the elastic buckling of cylindrical shells made of isotropic material under pure torsion. Yamaki et al. [51] conducted precise experimental tests on the postbuckling performances of clamped cylindrical shell subjected to pure torsion. Shokrieh et al. [52] adopted finite element method to determine the critical torsional buckling load of a cylindrical shell.

Although studies have been done on graphene reinforced composites and structures, relatively less work has been found on torsional buckling behaviours of graphene reinforced functionally graded cylindrical shells with cutouts. Therefore, this paper will implement numerical simulation to comprehensively investigate the torsional buckling behaviours of a functionally graded cylindrical shell as shown in Fig. 1. L, R and t are the length, radius and thickness of the cylindrical shell, respectively. It should be noted that due to the limitation of the current manufacture technology, the fabrication of a FGM structure with continuous variation of GPL dispersion in the thickness direction is challenging. The functionally graded cylindrical shells will be achieved by stacking a number of layers in the thickness direction. GPLs are uniformly distributed in each individual layer while the GPL concentration varies from layer to layer according to prescribed distribution patterns as shown in Fig. 2.

2. Effective mechanical properties of GPL/Polymer composites

The functionally graded cylindrical shell reinforced with GPLs is consisted of a number of layers in the thickness direction. GPLs are uniformly distributed in each individual layer while the GPL concentration varies from layer to layer. According to the variation of the concentration, four distribution patterns as shown in Fig. 2 are considered. A homogenous dispersion of GPLs with constant concentration along the entire thickness direction is prescribed in Pattern 1. Patterns 2 and 3 correspond to symmetric GPL distribution. GPLs concentration increases linearly from inner and outer layers to the middle layers for pattern 2 and vice versa for pattern 3. For pattern 4, the GPL concentration increases linearly from inner layer to outer layer. It should be noted that the average GPL weight fraction, which is denoted as f_{GPL}, remains the same for the four distribution patterns. In what follows, the GPLs weight fraction in ith layer for the four distribution patterns are given as

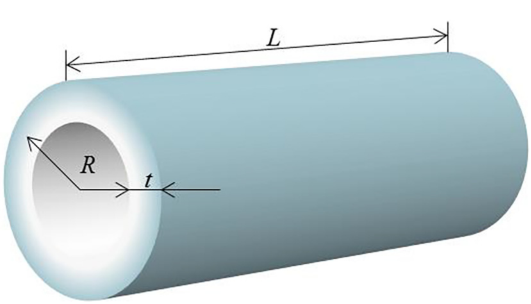

Fig. 1. Geometry of functionally graded cylindrical shell.

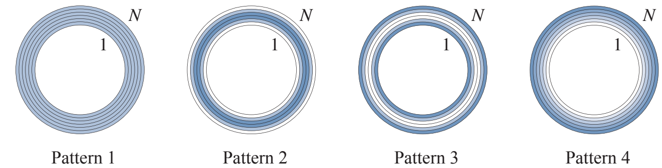

Fig. 2. Four GPL distribution patterns.

$$\text{Pattern 1: } f_i = f_{GPL} \tag{1}$$

$$\text{Pattern 2: } \begin{cases} f_i = (i-1)\frac{4f_{GPL}}{N-2} & i \leqslant \frac{N}{2} \\ f_i = 2f_{GPL} - \left(i-\frac{N}{2}-1\right)\frac{4f_{GPL}}{N-2} & i > \frac{N}{2} \end{cases} \tag{2}$$

$$\text{Pattern 3: } \begin{cases} f_i = 2f_{GPL} - (i-1)\frac{4f_{GPL}}{N-2} & i \leqslant \frac{N}{2} \\ f_i = \left(i-\frac{N}{2}-1\right)\frac{4f_{GPL}}{N-2} & i > \frac{N}{2} \end{cases} \tag{3}$$

$$\text{Pattern 4: } f_i = (i-1)\frac{2f_{GPL}}{N-1} \tag{4}$$

For each individual layer, the Young's modulus of the GPL reinforced composite can be determined by Halpin-Tsai micromechanics model, whose accuracy was validated by Rafiee's experiments [17]. For the two-phase material, the effective Young's modulus of the composite can be approximated as [53,54]

$$E_C = \frac{3}{8}\frac{1+\xi_L\eta_L V_{GPL}}{1-\eta_L V_{GPL}} \times E_M + \frac{5}{8}\frac{1+\xi_W\eta_W V_{GPL}}{1-\eta_W V_{GPL}} \times E_M \tag{5}$$

$$\eta_L = \frac{(E_{GPL}/E_M)-1}{(E_{GPL}/E_M)+\xi_L}, \quad \eta_W = \frac{(E_{GPL}/E_M)-1}{(E_{GPL}/E_M)+\xi_W} \tag{6}$$

where E_M and E_{GPL} are the Young's moduli of epoxy matrix and GPLs, respectively. ξ_L and ξ_W are two parameters characterizing the geometry of GPL nanofillers, which could be expressed as

$$\xi_L = 2\left(\frac{l_{GPL}}{t_{GPL}}\right), \quad \xi_W = 2\left(\frac{w_{GPL}}{t_{GPL}}\right) \tag{7}$$

where l_{GPL}, w_{GPL} and t_{GPL} represent the average length, width and thickness of GPL nanofillers. V_{GPL} in Eq. (5) denotes the GPL volume fraction, which can be derived as

$$V_{GPL} = \frac{f_{GPL}}{f_{GPL} + (\rho_{GPL}/\rho_M)(1-f_{GPL})} \tag{8}$$

where ρ_{GPL} and ρ_M are the mass densities of GPL and the polymer matrix, respectively. Using rule of mixture, the Poisson's ratio of the nanocomposites is approximated as $\nu_C = \nu_{GPL}V_{GPL} + \nu_M(1-V_{GPL})$, where ν_{GPL} and ν_M are the Poisson's ratios of the GPL and the polymer matrix, respectively.

3. Computation of torsional buckling load

When a cylindrical shell is subjected to a pure torsion in the loop direction, the governing equation for the structure before buckling can be expressed as

$$\boldsymbol{K}^{MN}\boldsymbol{q}^M = 0 \tag{9}$$

where $\boldsymbol{K}^{MN}$ is the tangent stiffness matrix after applying the torsion, $\boldsymbol{q}^M$ is the displacement vector, and the subscripts M and N denote the degrees of freedom of the structures. Before buckling, the cylindrical shell is in static state and the induced deformation can be neglected compared to the dimensions of the structure. Eq. (9) has trivial solution only, i.e. $\boldsymbol{q}^M = 0$. However, as the loading increases to a critical value, the cylindrical shell wrinkles suddenly and demonstrates significantly reduced torsional stiffness. Theoretically, the tangent stiffness matrix $\boldsymbol{K}^{MN}$ becomes singular and non-trivial solution to Eq. (9) can be found,